Gene symbol	Log ratio	Relative expression in skeletal muscle
Rnf40	-0.0068	63.48
Rnf20	-0.0142	4.64
Stub1	-0.0215	1238.83
Brca1	-0.0226	9.09
Rnf115	-0.0227	2630.99
Ttc3	-0.0314	ND
Hecw2	-0.035	6.32
Arih1	-0.0382	890.86
Wwp1	-0.0414	2440.56
Hectd1	-0.0437	1595.0
Klhl21	-0.0508	115.44
Cul3	-0.0728	1003.16
Ube3b	-0.0869	2396.53
Rffl	-0.096	128.51
Huwe1	-0.1139	14.48
Trim24	-0.1547	153.49
Trip12	-0.1884	6.85
Ubr3	-0.2096	2333.04
Herc2	-0.2297	4.64
Nedd4	-0.2393	6448.4
Syvn1	-0.2795	122.73
Ubr4	-0.2987	517.89
Trim32	-0.3009	285.18
Uhrf1	-0.3189	21.33
Lrsam1	-0.5057	155.92
Cbl	-0.6542	201.25
Rnf135	-0.7412	46.57

Supplemental Table 1. E3 ubiquitin ligase genes whose expression was found to be down-regulated in gastrocnemius of STZ diabetic mice by microarray analysis as well as the relative expression of these genes in skeletal muscle revealed by analysis of the BioGPS database. Log ratio indicates $\log_{10}$ of the ratio of the expression level in STZ diabetic mice to that in control mice. Eight genes with the highest relative expression level in skeletal muscle are shown in red.

Gene	Primer
36b4	FWD: GAGGAATCAGATGAGGATATGGGA
	REV: AAGCAGGCTGACTTGGTTGC
Klf15	FWD: ACCGAAATGCTCAGTGGGTTACCTA
	REV: GGAACAGAAGGCTTGCGAGTCA
Wwp1	FWD: AGAATGGAGACCCTGCAACAAG
	REV: GCAGGAGTTGGGAACAACAGTA
Atrogin1	FWD: GCAAACACTGCCACATTCTCTC
	REV: CTTGAGGGGAAAGTGAGACG
Murf1	FWD: GCTGGTGGAAAACATCATTGACAT
	REV: CATCGGGTGGCTGCCTTT
Foxo3a	FWD: CAGGCTCCTCACTGTATTCAGCTA
	REV: CATTGAACATGTCCAGGTCCAA
Prodh	FWD: TCATCAGTGCCCGCACCTAC
	REV: TGCAGTGAGCTTAATGGCTGAGA
Tdo2	FWD: TGCTCAAGGTGATAGCTCGGA
	REV: AGGAGCTTGAAGATGACCACCA

Supplemental Table 2. Primer sequences used in quantitative RT-PCR analysis.

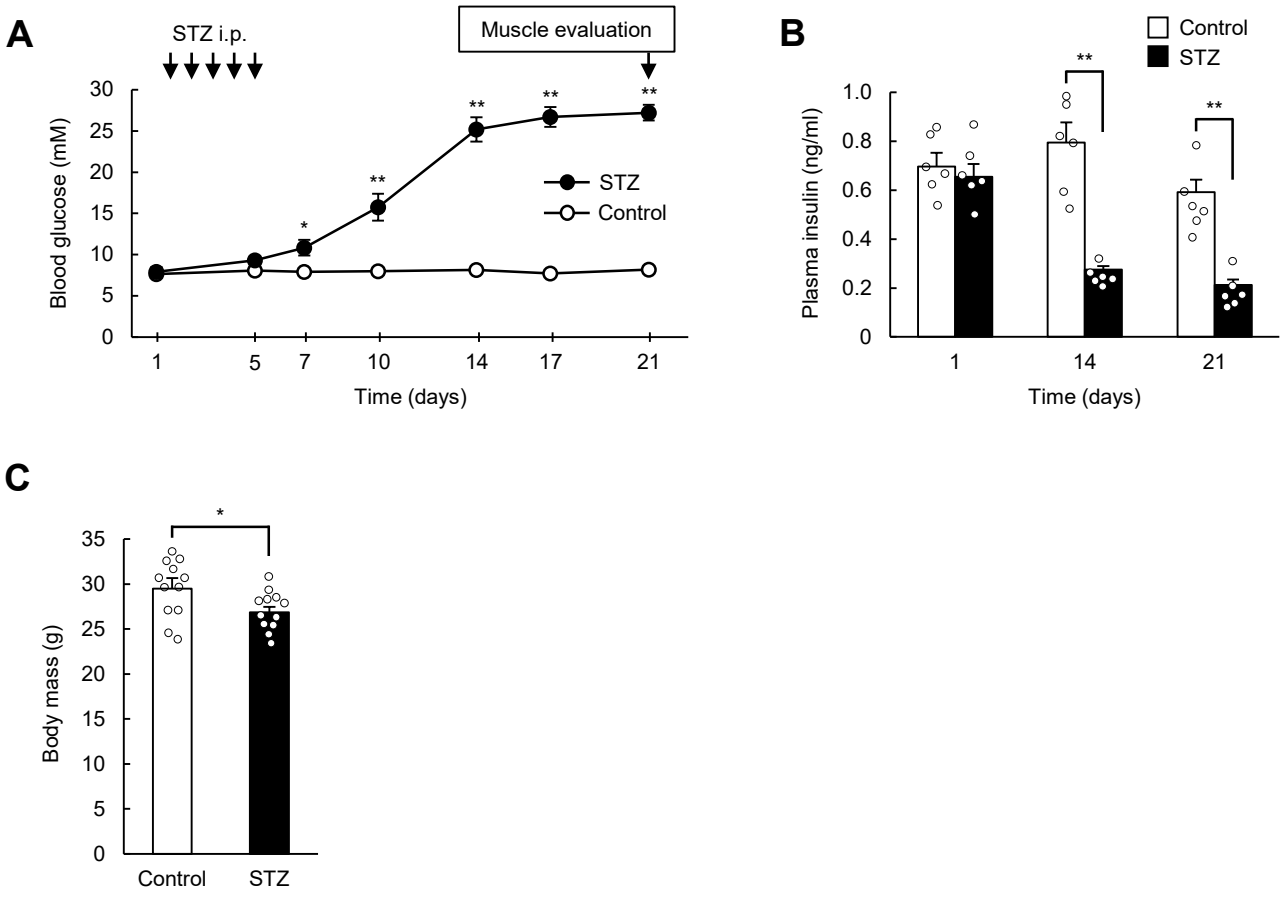

Supplemental Figure 1. Mouse model of STZ-induced diabetes. (**A** and **B**) Blood glucose (A; n = 6) and plasma insulin (B; n = 6) concentrations of mice at the indicated times after the onset of intraperitoneal (i.p.) injection of STZ or vehicle (Control) for five consecutive days at 10 weeks of age. (**C**) Body mass of mice as in (A) at 21 days after the onset of STZ or vehicle injection. n = 12. All quantitative data are means ± SEM for the indicated numbers of mice. **P* < 0.05, ***P* < 0.01 versus the corresponding value for control mice or for the indicated comparisons. Unpaired *t* test (C) or 2-way ANOVA with Bonferroni post-hoc test (A and B).

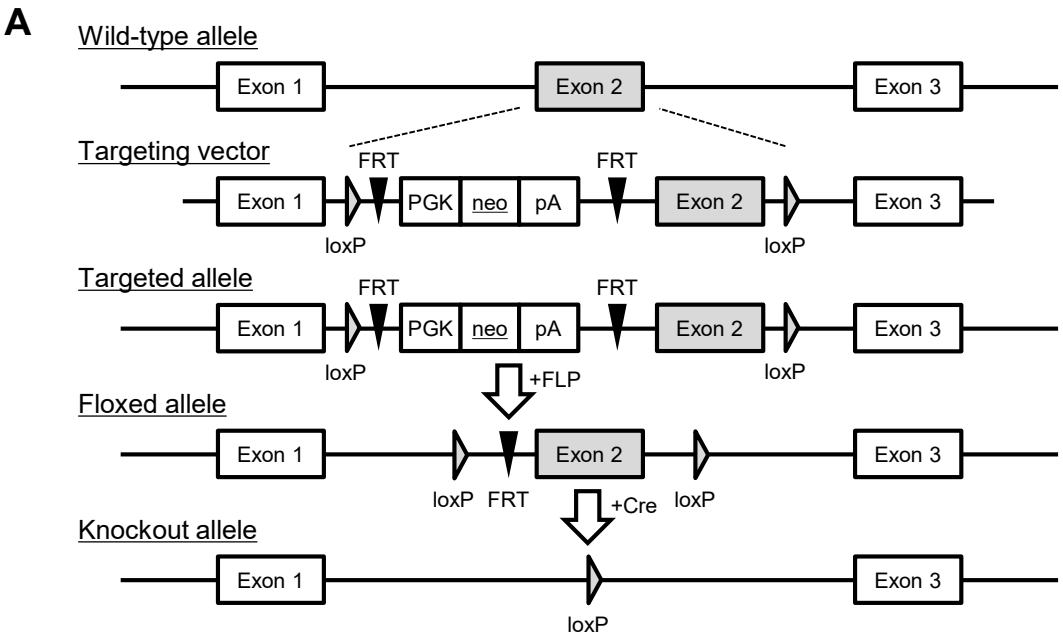

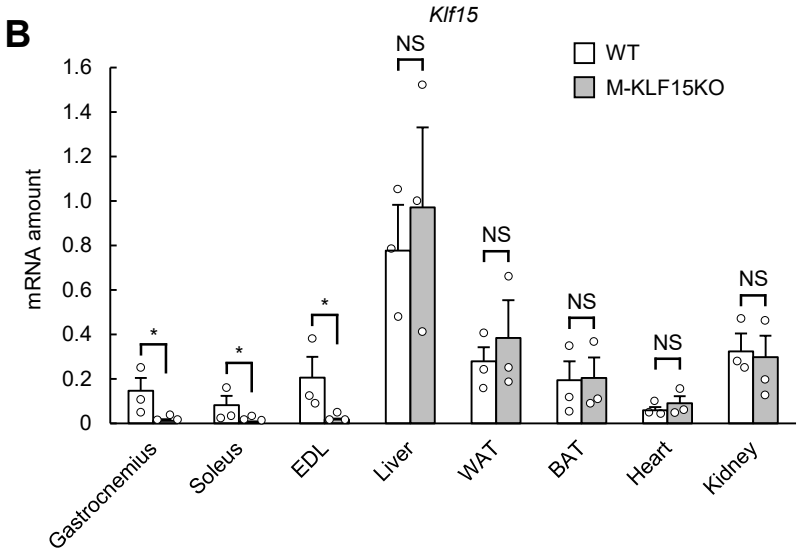

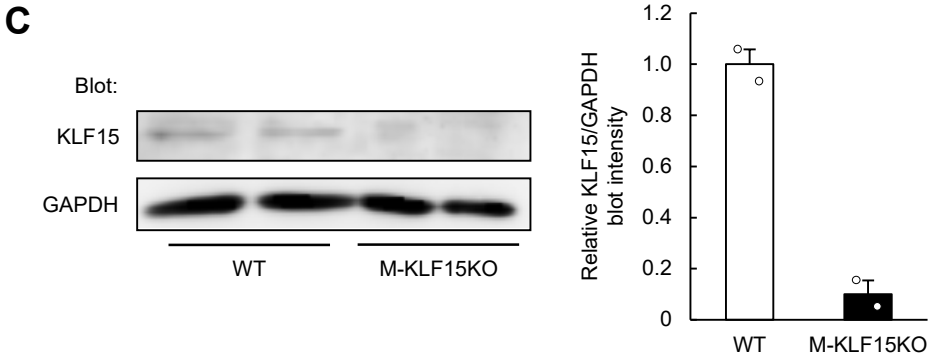

Supplemental Figure 2. Generation of M-KLF15KO mice. (**A**) Structure of the mouse *Klf15* genomic locus and the targeting vector for deletion of *Klf15*. (**B**) Quantitative RT-PCR analysis of the tissue distribution of *Klf15* mRNA in WT and M-KLF15KO mice at 8 weeks of age. WAT and BAT, white and brown adipose tissue, respectively. n = 3. (**C**) Immunoblot analysis of KLF15 in soleus muscle (nuclear fraction from 3 mice was loaded on one lane) of mice as in (B). n = 2. All quantitative data are means ± SEM for the indicated numbers of mice. **P* < 0.05; NS, not significant. Unpaired *t* test (B).

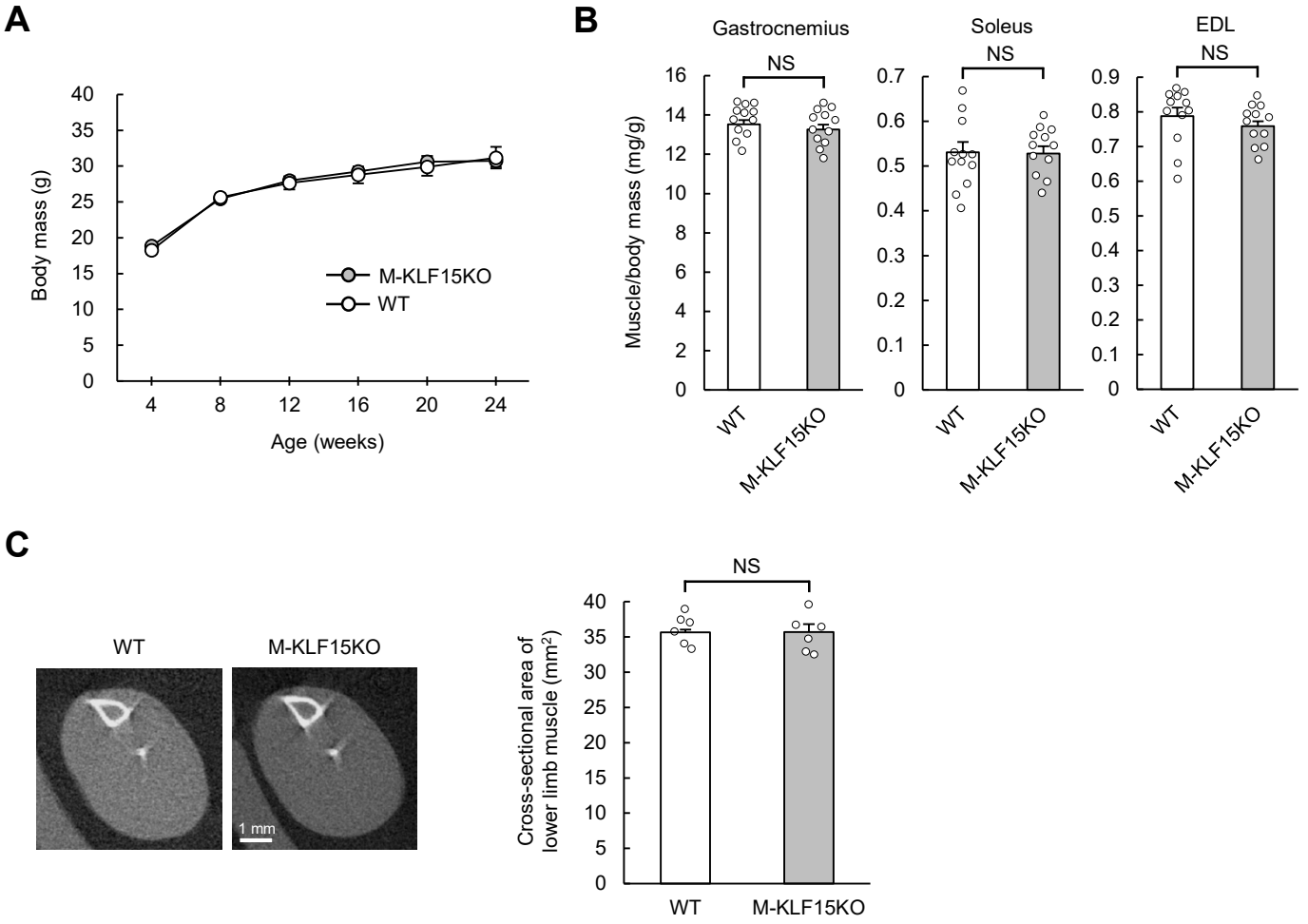

Supplemental Figure 3. Characterization of M-KLF15KO mice. (**A**) Time course of body mass in WT (n = 7) and M-KLF15KO mice (n = 12). (**B** and **C**) Skeletal muscle mass (B; n = 12) and cross-sectional area of lower limb muscle as determined by computed tomography (C; n = 6) in WT and M-KLF15KO mice at 10 weeks of age. All quantitative data are means ± SEM for the indicated numbers of mice. NS, not significant. Unpaired *t* test (B and C).

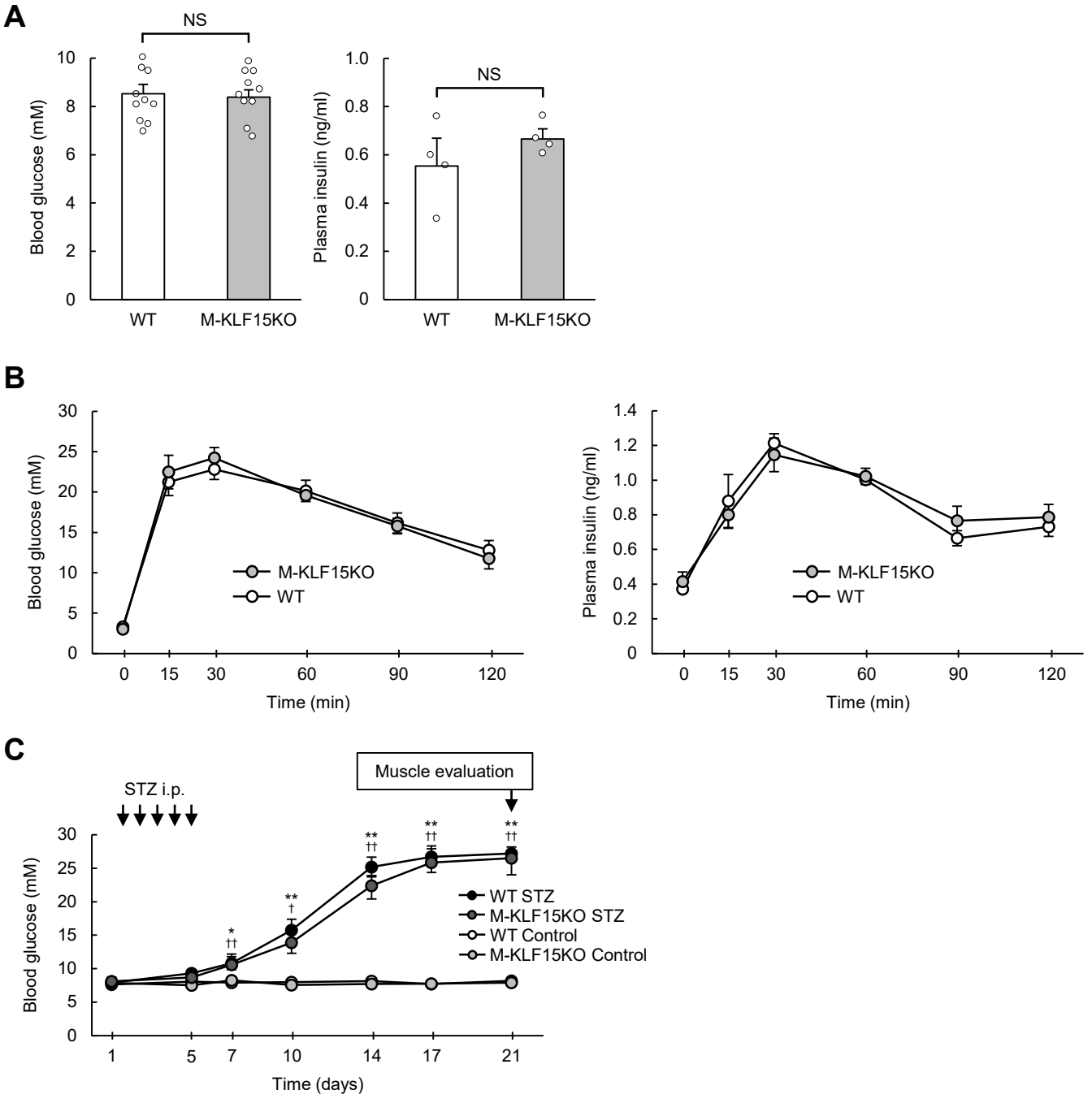

Supplemental Figure 4. Blood glucose and plasma insulin concentrations as well as STZ-induced diabetes in M-KLF15KO mice. (**A** and **B**) Blood glucose and plasma insulin levels in WT and M-KLF15KO mice at 8 weeks of age under the static condition (A; n = 10) and 20 weeks of age during an intraperitoneal glucose tolerance test (B; n = 6). (**C**) Blood glucose concentration of WT and M-KLF15KO mice at the indicated times after the onset of STZ (or vehicle) injection for the induction of diabetes at 10 weeks of age. n = 6. All quantitative data are means ± SEM for the indicated numbers of mice. **P* < 0.05, ***P* < 0.01 for STZ versus vehicle control in WT mice; †*P* < 0.05, ††*P* < 0.01 for STZ versus vehicle control in M-KLF15KO mice. NS, not significant. Unpaired *t* test (A) or 2-way ANOVA with Bonferroni post-hoc test (C).

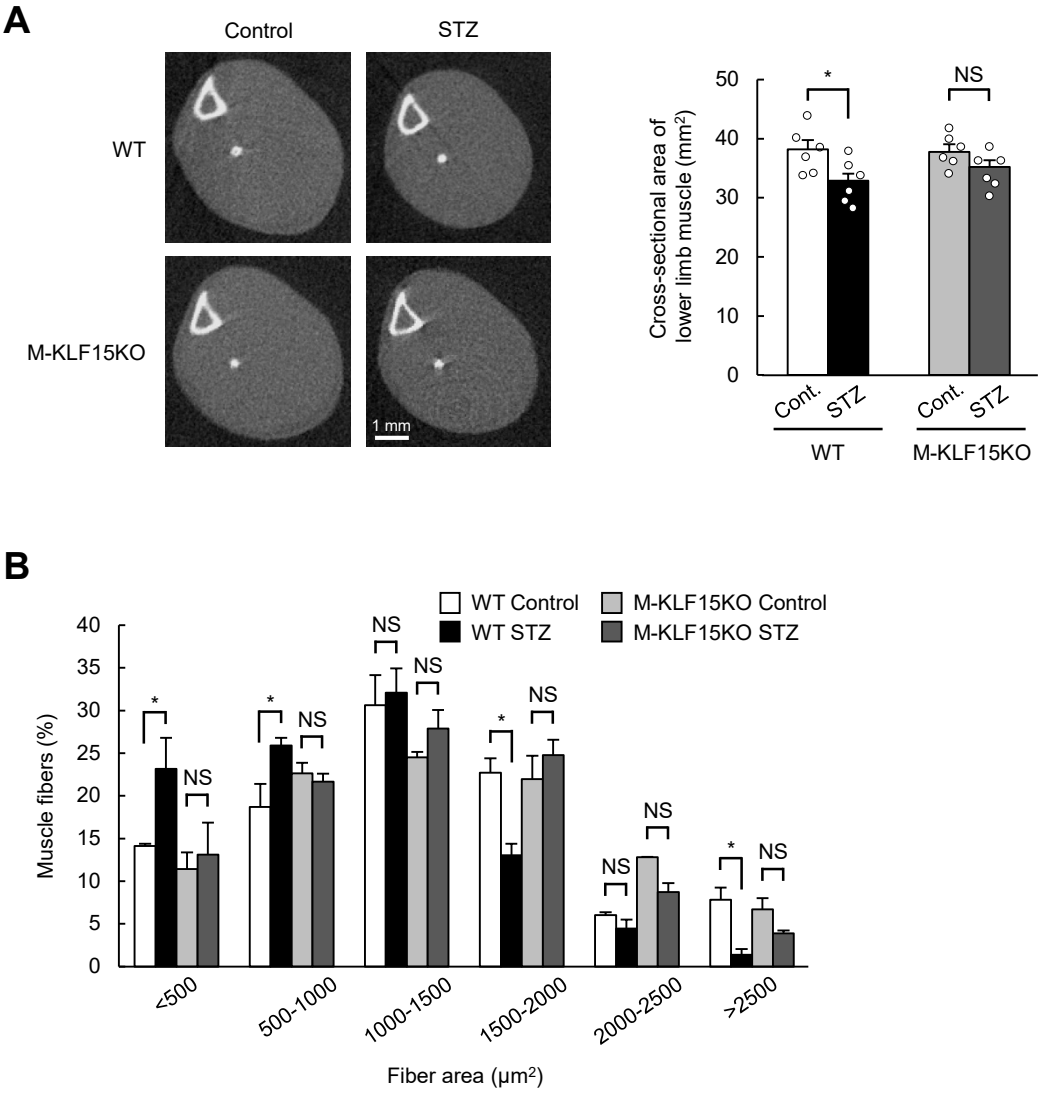

Supplemental Figure 5. Prevention of STZ-induced muscle atrophy in M-KLF15KO mice. (**A**) Cross-sectional area of lower limb muscle as evaluated by computed tomography in WT and M-KLF15KO mice at 21 days after the onset of STZ (or vehicle) injection for the induction of diabetes. Representative images and quantitative data from 6 mice are shown in left and right panels, respectively. (**B**) Distribution of muscle fiber area for EDL as evaluated by histology in WT and M-KLF15KO mice at 21 days after the onset of STZ or vehicle (Control) injection. All quantitative data are means ± SEM for the indicated numbers of mice. *$P < 0.05$; NS, not significant. 2-way ANOVA with Bonferroni post-hoc test (A and B).

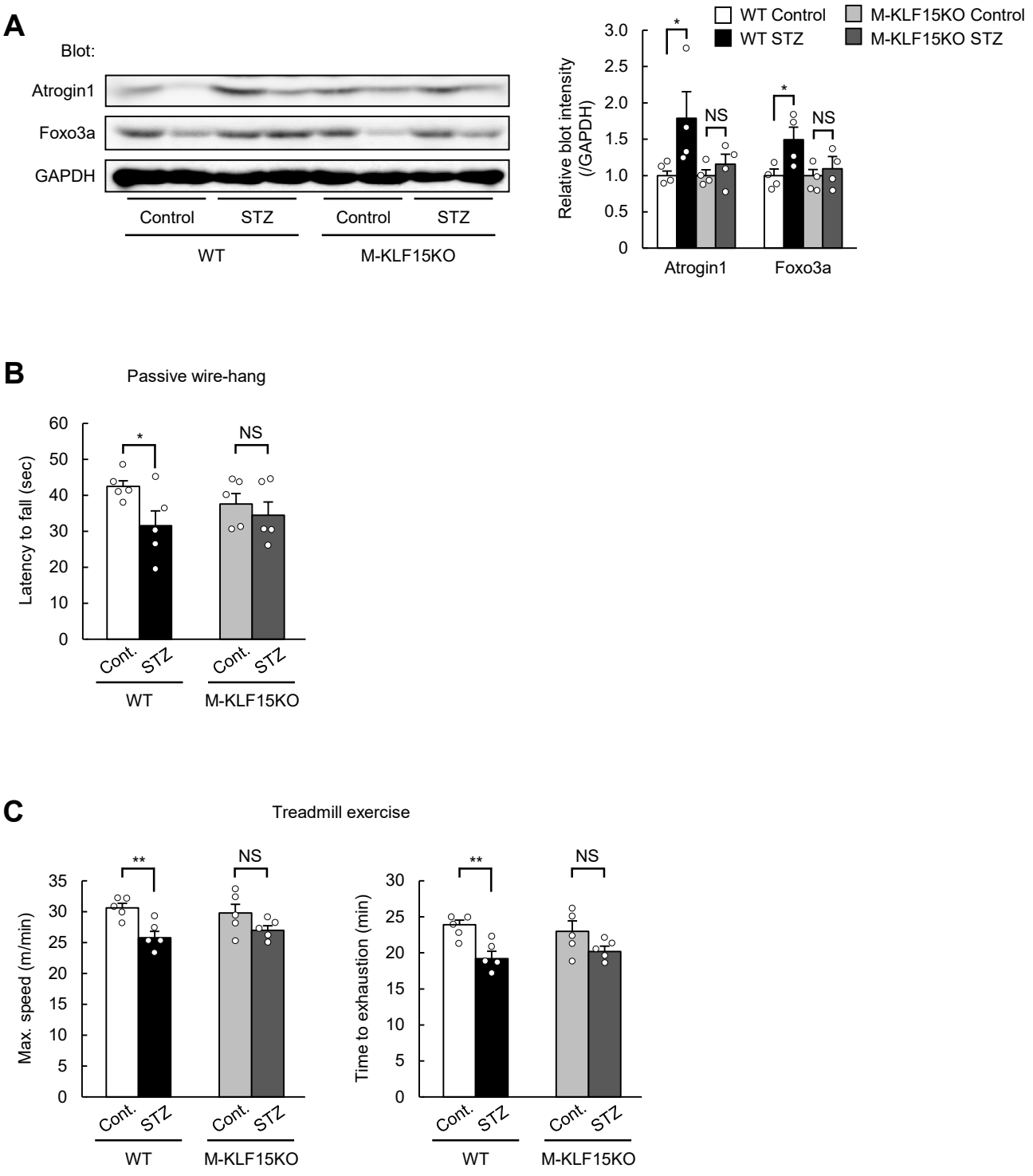

Supplemental Figure 6. Prevention of STZ-induced alteration of gene expression and decrease in muscle function in M-KLF15KO mice. (**A**) Immunoblot analysis of Atrogin1 and Foxo3a in gastrocnemius muscle in WT and M-KLF15KO mice at 21 days after the onset of STZ or vehicle (Control) injection. A representative blot and quantitative data (n = 4) are shown in left and right panels, respectively. (**B** and **C**) Latency to fall in passive wire-hang test (B; n = 5) and maximal speed, time to exhaustion, and distance to exhaustion evaluated by graded treadmill exercise protocol (C; n = 5) in WT and M-KLF15KO mice at 21 days after the onset of STZ or vehicle (Control) injection. All quantitative data are means ± SEM for the indicated numbers of mice. **P* < 0.05, ***P* < 0.01; NS, not significant. 2-way ANOVA with Bonferroni post-hoc test (A to C).

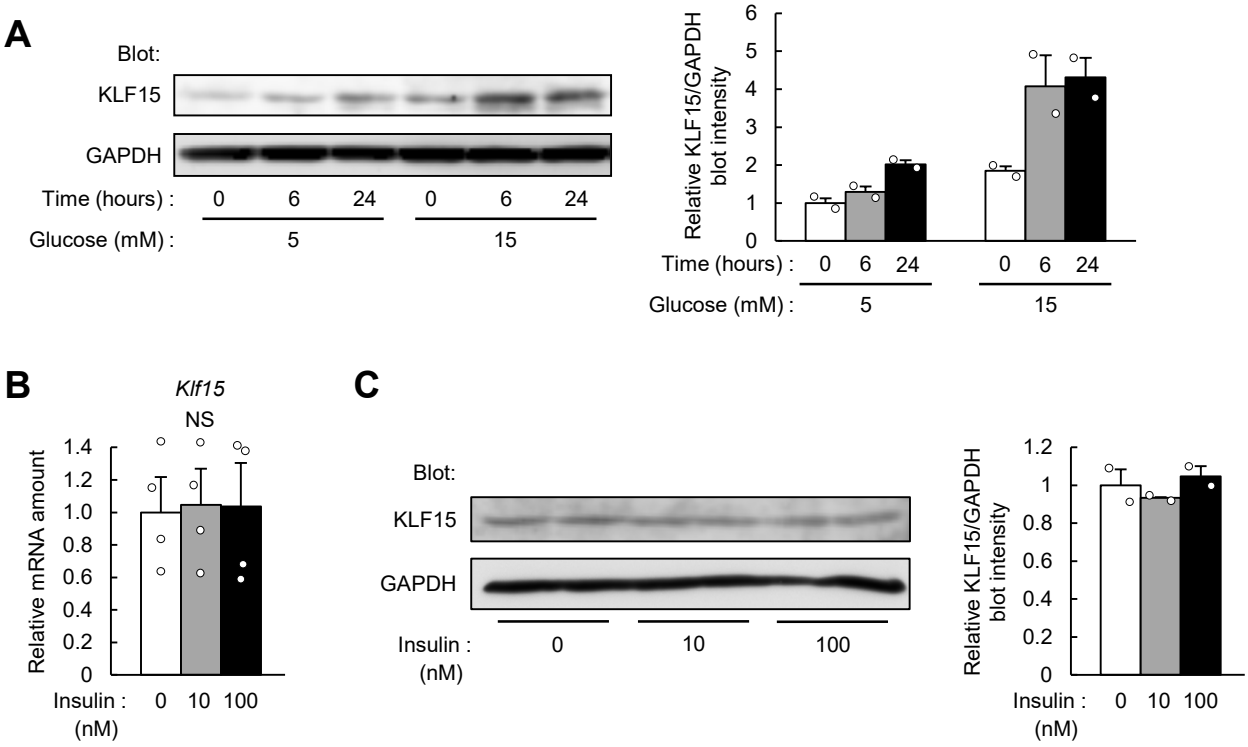

Supplemental Figure 7. Effects of glucose and insulin on KLF15 expression in C2C12 myotubes. (**A**) Immunoblot analysis of KLF15 in C2C12 myotubes exposed to 5 or 15 mM glucose for the indicated times. n = 2. (**B** and **C**) Quantitative RT-PCR analysis of *Klf15* mRNA (B; n = 4) and immunoblot analysis of KLF15 protein (C; n = 2) in C2C12 myotubes exposed to the indicated concentrations of insulin for 24 hours. All quantitative data are means ± SEM for the indicated numbers of independent experiments. NS, not significant. 2-way ANOVA with Bonferroni post-hoc test (B).

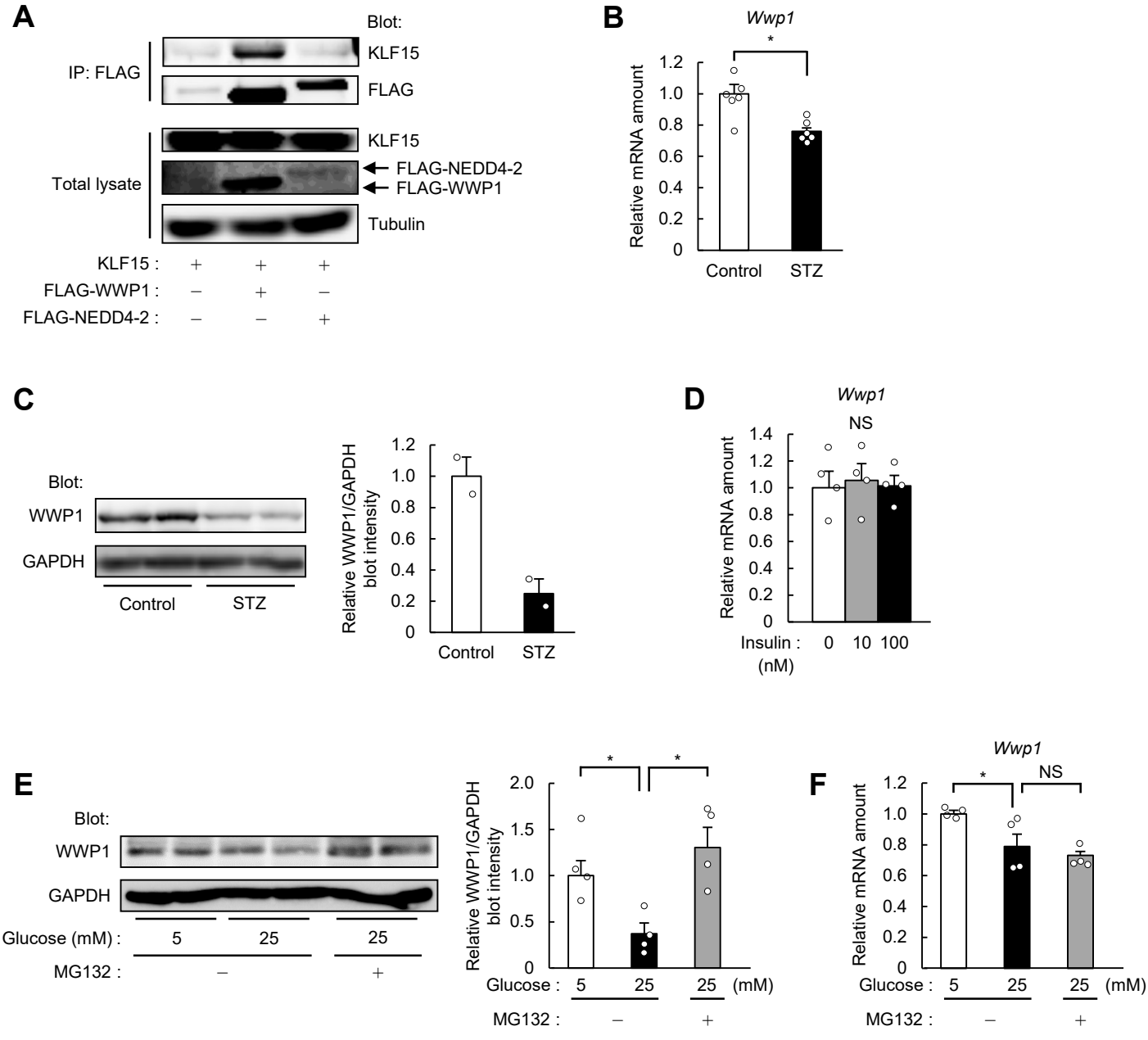

Supplemental Figure 8. Expression of WWP1 and its interaction with KLF15. (**A**) COS-7 cells transfected with vectors for KLF15, FLAG-WWP1, or FLAG–NEDD4-2 were subjected to immunoprecipitation with antibodies to FLAG. The resulting precipitates as well as the original cell lysates were subjected to immunoblot analysis as indicated. α-Tubulin was examined as a loading control. A representative data from three independent experiments is shown. (**B** and **C**) Quantitative RT-PCR analysis of *Wwp1* mRNA in gastrocnemius (B; n = 6) and immunoblot analysis of WWP1 protein in soleus muscle (nuclear fraction from 3 mice was loaded on one lane) (C; n = 2) of control and STZ diabetic mice. (**D**) Quantitative RT-PCR analysis of *Wwp1* mRNA in C2C12 myotubes exposed to the indicated concentrations of insulin for 24 hours. n = 4. (**E** and **F**) Immunoblot analysis of WWP1 protein (E) and quantitative RT-PCR analysis of *Wwp1* mRNA (F; n = 4) in myotubes exposed to 5 or 25 mM glucose in the absence or presence of 15 μM MG132 for 24 hours. In **E**, a representative blot and quantitative data (n = 4) are shown in left and right panels, respectively. All quantitative data are means ± SEM for the indicated numbers of mice (B and C) or independent experiments (D to F). *P < 0.05; NS, not significant. Unpaired t test (B) or 2-way ANOVA with Bonferroni post-hoc test (D to F).

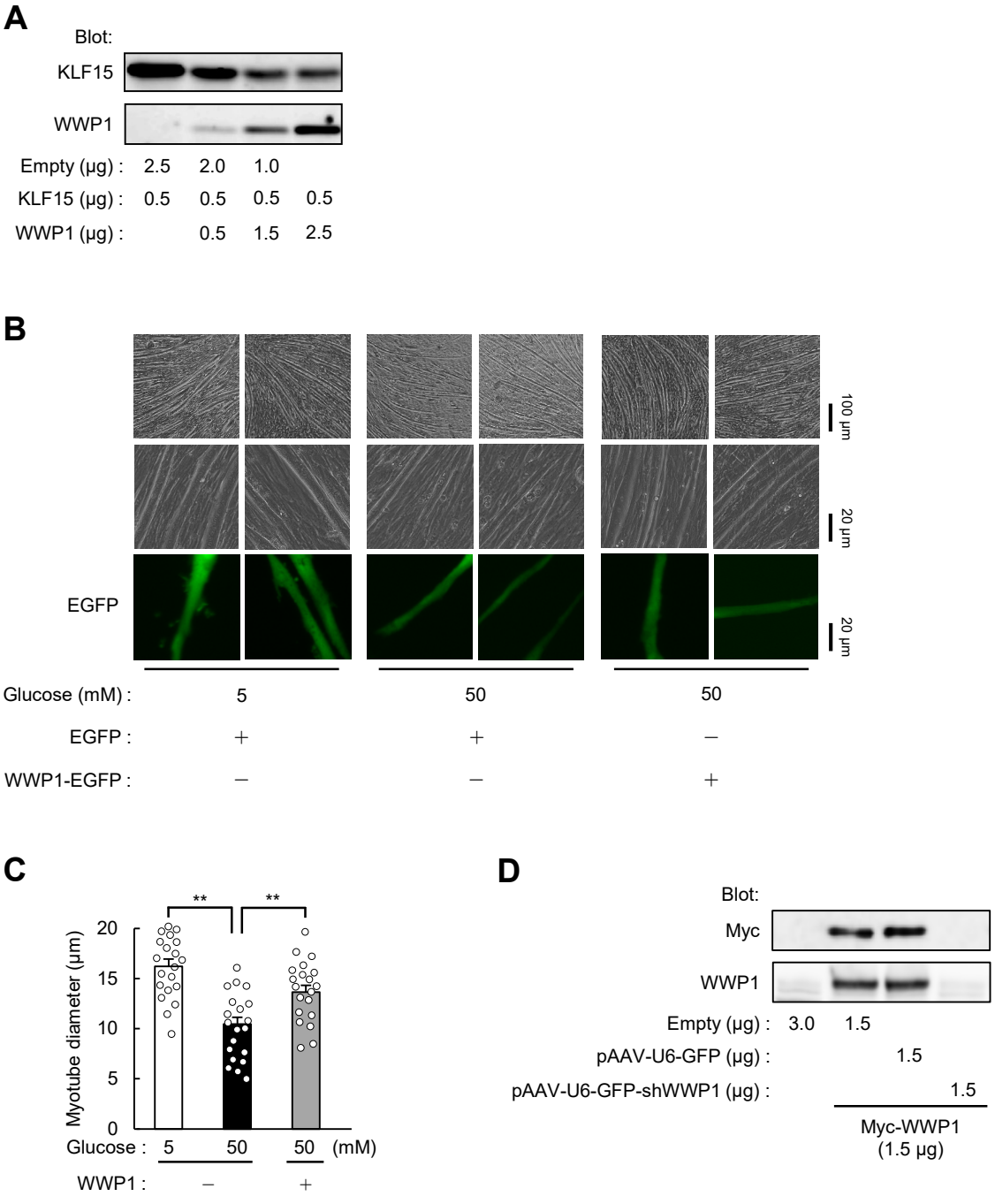

Supplemental Figure 9. Effect of WWP1 on KLF15 expression and high glucose-induced myotube atrophy. (**A**) Immunoblot analysis of KLF15 and WWP1 in COS-7 cells transfected with expression vectors for these proteins or empty vector as indicated. (**B**) Phase-contrast and fluorescence microscopic detection of EGFP-positive C2C12 myotubes exposed to the indicated concentrations of glucose and transfected with the indicated vectors. (**C**) Diameter of EGFP-positive C2C12 myotubes determined from images as in (B). n = 20. (**D**) Immunoblot analysis of WWP1 in HEK 293 cells transfected with an expression vector for Myc epitope–tagged WWP1 as well as with pAAV-U6-GFP or pAAV-U6-GFP-shWWP1 (encoding WWP1 shRNA) as indicated. All quantitative data are means ± SEM for the indicated numbers of independent experiments. ***P* < 0.01. 2-way ANOVA with Bonferroni post-hoc test (C).

A

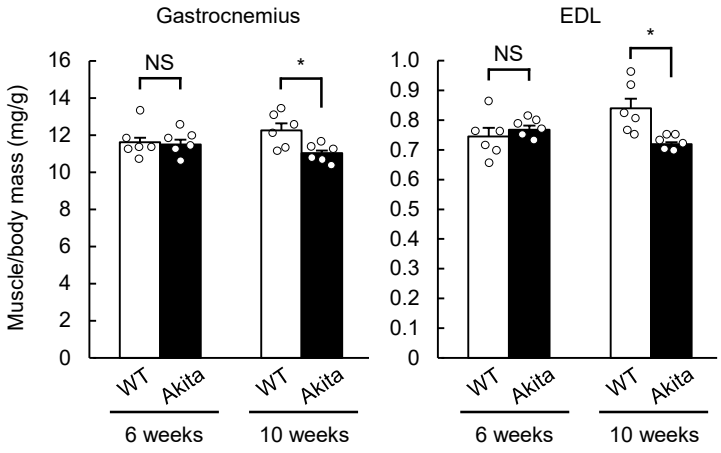

Supplemental Figure 10. Skeletal muscle mass of WT and Akita mice. (**A**) Ratio of gastrocnemius or EDL muscle mass to body mass of WT and Akita mice at 6 and 10 weeks of age. n = 6. All quantitative data are means ± SEM for the indicated numbers of mice. *P < 0.05; NS, not significant. 2-way ANOVA with Bonferroni post-hoc test (A).

Figure 1C

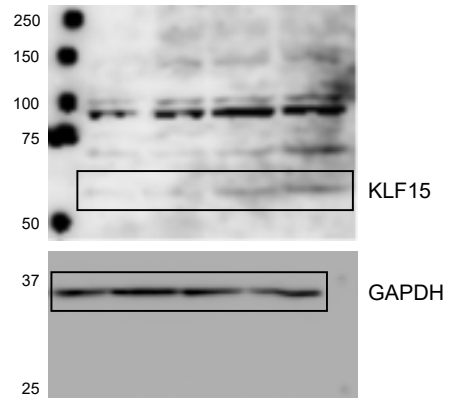

Figure 2A

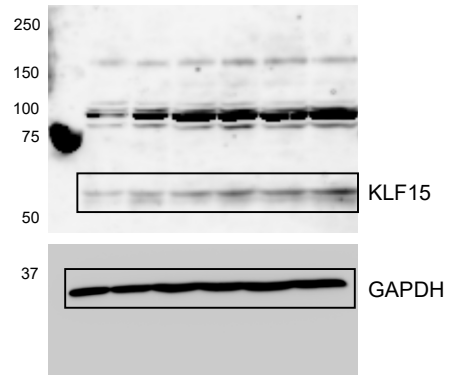

Figure 2D

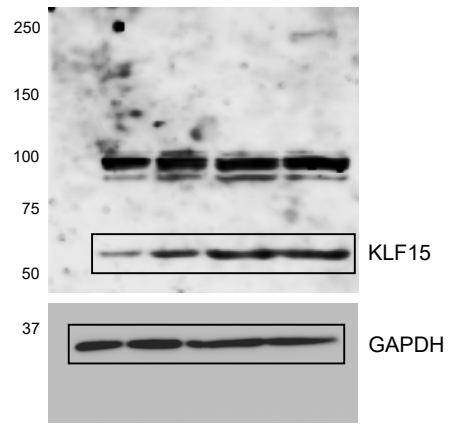

Figure 2E

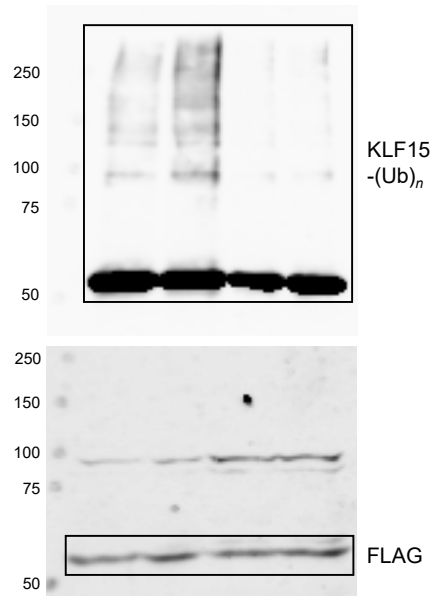

Figure 3B

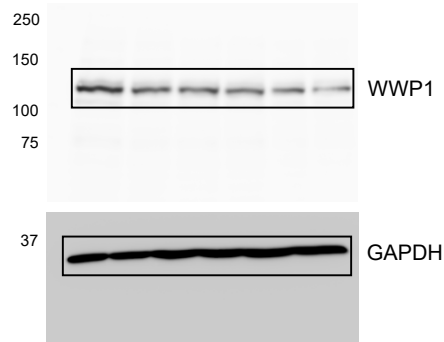

Figure 3C

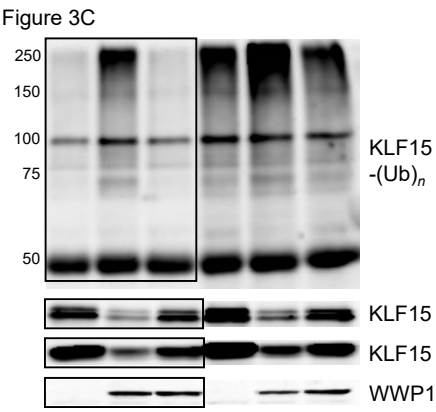

Figure 4B

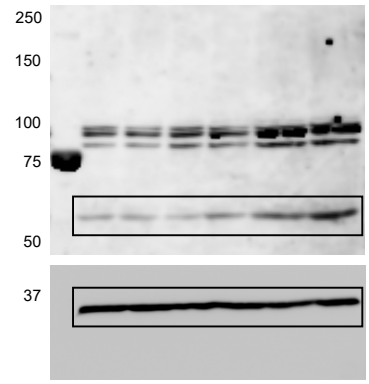

Figure 6B

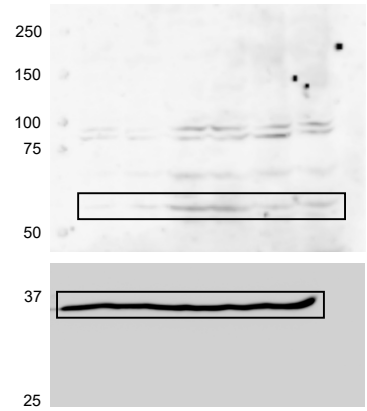

Figure S2C

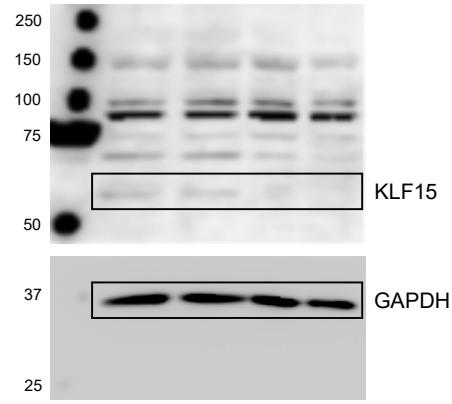

Figure S6A

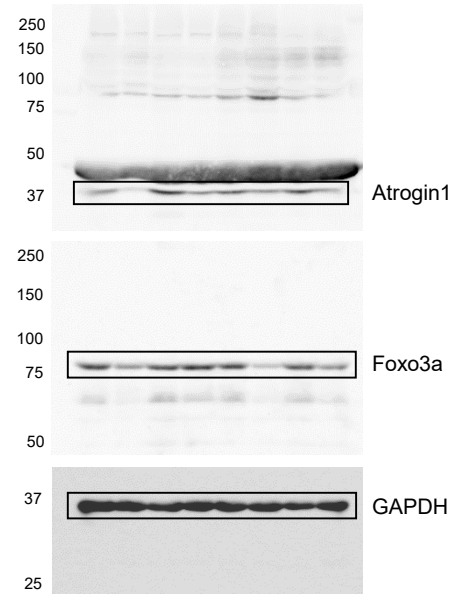

Figure S7A

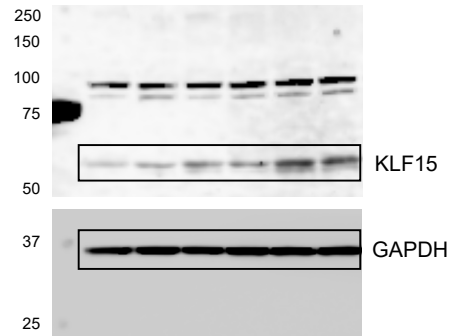

Figure S7C

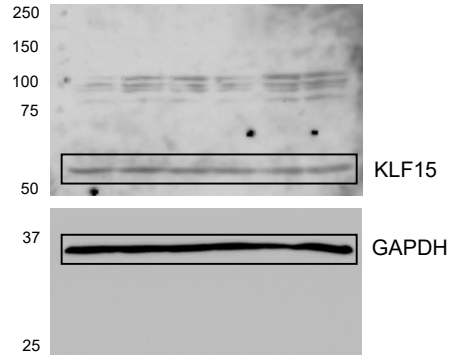

Figure S8C

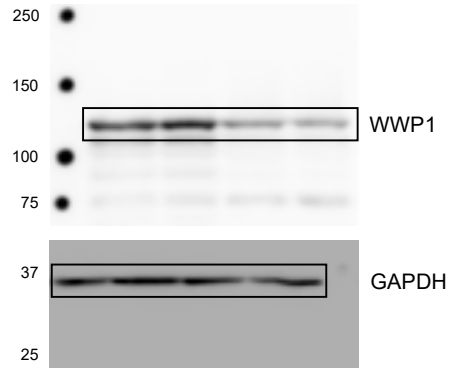

Figure S8E

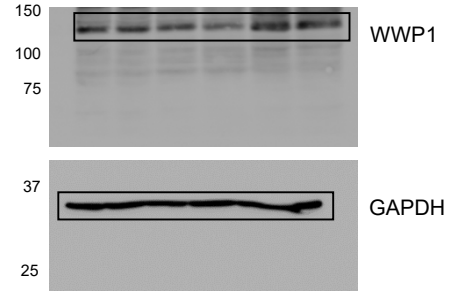

Figure S9D

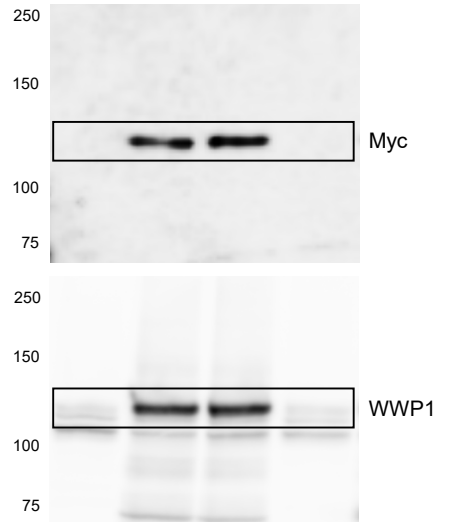

Supplemental Figure 11. Uncropped blot images. Black box indicates area that was cropped and displayed in the indicated figures.